

# CH<sub>3</sub>ReO<sub>3</sub> on $\gamma$ -Al<sub>2</sub>O<sub>3</sub>: Understanding Its Structure, Initiation, and Reactivity in Olefin Metathesis\*\*

Alain Salameh, Jérôme Joubert, Anne Baudouin, Wayne Lukens, Françoise Delbecq, Philippe Sautet,\* Jean Marie Basset,\* and Christophe Copéret\*

Understanding the structure of catalytically active sites at a molecular level is still a challenge in heterogeneous catalysis. Surface organometallic chemistry (SOMC) has investigated ways to generate well-defined heterogeneous catalysts through a molecular approach to better understand these systems.<sup>[1]</sup> This has already yielded several efficient catalysts for olefin conversion processes (polymerization, hydrogenation, metathesis),<sup>[1–3]</sup> and even processes to convert alkanes at low temperatures.<sup>[4]</sup> In the specific field of olefin metathesis, we have developed a series of well-defined silica-supported metal alkylidene complexes,<sup>[5]</sup> which have shown unprecedented performance compared to both homogeneous and heterogeneous catalysts.

However, industrial processes typically rely on simpler catalytic systems, and one of the simplest and most efficient heterogeneous catalysts for olefin metathesis derived from SOMC is based on CH<sub>3</sub>ReO<sub>3</sub><sup>[6]</sup> supported on Lewis acidic supports such as silica alumina,<sup>[7,8]</sup> alumina,<sup>[9]</sup> niobia,<sup>[10]</sup> or zeolites.<sup>[11]</sup> Recent investigations have shown that CH<sub>3</sub>ReO<sub>3</sub> is grafted to silica alumina mainly through coordination by Lewis acid/Lewis base interaction.<sup>[8]</sup> However, the structure

of the so-called active site remains elusive, and the mechanism of formation of the expected propagating carbene species is unknown. Despite numerous studies, a question remains: is the methyl group of CH<sub>3</sub>ReO<sub>3</sub> involved in the formation of the initial carbene?<sup>[10,12,13]</sup>

Through a combination of spectroscopic (IR, NMR, and EXAFS), reactivity, and molecular modeling studies,<sup>[14,15]</sup> we show below that CH<sub>3</sub>ReO<sub>3</sub> reacts with  $\gamma$ -alumina partially dehydroxylated at 500 °C ( $\gamma$ -Al<sub>2</sub>O<sub>3-(500)</sub>) to produce mainly a coordination adduct at the Lewis acid sites of this support through its oxo ligand. However, this species is not active, and the active sites correspond to a minor species that results from C–H activation of the methyl ligand of CH<sub>3</sub>ReO<sub>3</sub> at reactive Al<sub>s</sub>–O sites of alumina to yield surface hydroxy groups (Al<sub>s</sub>OH) and a surface Re methylene complex, namely, [Al<sub>s</sub>CH<sub>2</sub>ReO<sub>3</sub>], which is the initiating center for the carbene species propagating olefin metathesis.

Under static vacuum, we sublimed CH<sub>3</sub>ReO<sub>3</sub> onto  $\gamma$ -Al<sub>2</sub>O<sub>3-(500)</sub> at room temperature, and the solid turned deep red. The IR spectrum (Figure 1) showed the appearance of two bands at 2995 and 2910 cm<sup>–1</sup>, associated with the symmetric and antisymmetric  $\nu$ (CH<sub>3</sub>) modes, along with two bands at 1390 and 1204 cm<sup>–1</sup> assigned to  $\delta$ (CH<sub>3</sub>). Moreover, the original Al–OH bands have been replaced by a broad band centered at 3531 cm<sup>–1</sup> (spanning between 3759 and 3184 cm<sup>–1</sup>), which probably corresponds to OH in a new environment (interaction with CH<sub>3</sub>ReO<sub>3</sub>).<sup>[15]</sup> Finally, a weak band at 1958 cm<sup>–1</sup>, attributed to Re=O harmonics, is also observed.

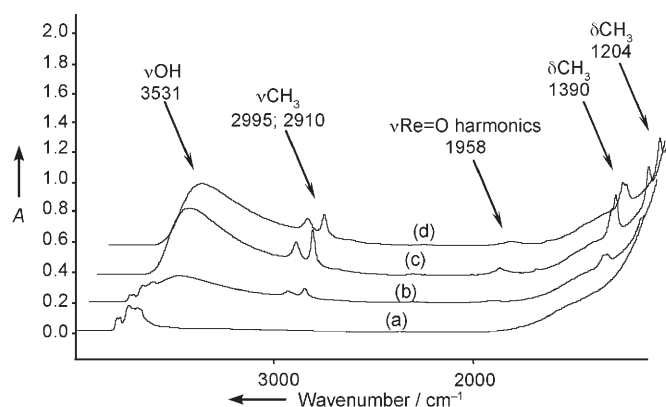


**Figure 1.** Monitoring the grafting of CH<sub>3</sub>ReO<sub>3</sub> on  $\gamma$ -Al<sub>2</sub>O<sub>3</sub> by IR spectroscopy. a)  $\gamma$ -Al<sub>2</sub>O<sub>3-(500)</sub> after calcination and treatment at 500 °C under vacuum (10<sup>–5</sup> Torr), b) 5 min after breaking the seal isolating CH<sub>3</sub>ReO<sub>3</sub> from  $\gamma$ -Al<sub>2</sub>O<sub>3-(500)</sub>, c) after sublimation of CH<sub>3</sub>ReO<sub>3</sub> onto  $\gamma$ -Al<sub>2</sub>O<sub>3-(500)</sub> and desorption, and d) after evacuation at 10<sup>–5</sup> Torr for 2 h.

[\*] Dr. J. Joubert, Dr. F. Delbecq, Dr. P. Sautet  
Laboratoire de Chimie, Institut de Chimie de Lyon  
Ecole normale supérieure de Lyon, CNRS  
46 allée d'Italie, 69364 Lyon Cedex 07 (France)  
Fax: (+33) 472-728-860  
E-mail: philippe.sautet@ens-lyon.fr

Dr. A. Salameh, A. Baudouin, Dr. J. M. Basset, Dr. C. Copéret  
C2P2 Laboratoire de Chimie Organométallique de Surface  
UMR 5265 CNRS—ESCPE Lyon  
43 Bd du 11 Novembre 1918, 69616 Villeurbanne Cedex (France)  
Fax: (+33) 472-431-795  
E-mail: basset@cpe.fr  
coperet@cpe.fr

Dr. W. Lukens  
Chemical Sciences Division  
Lawrence Berkeley National Laboratory  
Berkeley, CA 94720 (USA)

[\*\*] A.S. is grateful to BASF for a graduate fellowship. We are all indebted to the BASF, CNRS, and ESCPE Lyon for financial support. This work was also sponsored in part by a grant to C.C. from the Agence Nationale pour la Recherche (ANR JC05 46372). We also thank Drs. V. Böhm, M. Röper, and D. Schneider for helpful discussions. Portions of this work were performed at the Lawrence Berkeley National Laboratory, which is operated by the US DOE under Contract No. DE-AC03-76SF00098, and at the Stanford Synchrotron Radiation Laboratory, a national user facility operated by Stanford University on behalf of the US DOE, Office of Basic Energy Sciences.

Supporting information for this article is available on the WWW under <http://www.angewandte.org> or from the author.

Elemental analysis of  $\text{CH}_3\text{ReO}_3/\gamma\text{-Al}_2\text{O}_{3-(500)}$  gave  $(3.8 \pm 0.1)$  wt % Re, which corresponds to 1.2 Re atoms per square nanometer. Thus, Re coverage is much lower than the number of OH groups on  $\gamma\text{-Al}_2\text{O}_{3-(500)}$  (4 OH per  $\text{nm}^2$ ). Note that 1) no  $\text{CH}_4$  evolved on grafting, and 2) reaction of  $\text{CH}_3\text{ReO}_3/\gamma\text{-Al}_2\text{O}_{3-(500)}$  with  $\text{H}_2\text{O}$  does not give  $\text{CH}_4$ ; these data show that the Re–C bond of  $\text{CH}_3\text{ReO}_3$  is not cleaved on grafting.

The extended X-ray absorption fine-structure (EXAFS) spectroscopic data are consistent with a Re center surrounded by four direct neighbors: 1 C at 2.16(2) and 3 O at 1.718(4) Å (Table 1 and Figure S1). The fit is improved by adding 1 O at a relatively short distance of 2.47(5) Å, along with 4 O at 3.47(4) and 2 Al at 3.11(3) Å. Considering the four direct neighbors, the Re–O and Re–C distances are elongated by about 1 and

**Table 1:** Re–X distances for  $\text{CH}_3\text{ReO}_3$  supported on  $\gamma\text{-Al}_2\text{O}_3$ , as measured by EXAFS ( $S_0^2 = 1$ ,  $\Delta E_0 = 5(1)$  eV).

Neighbor	No. of neighbors	Distance [Å]	$\sigma^2$ [Å <sup>2</sup> ]
O	2.8(2)	1.718(4)	0.0031(4)
$\text{CH}_3$	1	2.16(2)	0.006(2)
O	1	2.47(5)	0.013(3)
Al	2	3.11(3)	0.013 <sup>[a]</sup>
O	4	3.47(4)	0.013 <sup>[a]</sup>

[a] Constrained to equal the preceding variable.

5% compared to those of 1.704(3) and 2.063(2) Å in free  $\text{CH}_3\text{ReO}_3$ , respectively.<sup>[16]</sup> The structure of  $\text{CH}_3\text{ReO}_3$  supported on  $\gamma\text{-Al}_2\text{O}_{3-(500)}$  is thus largely unchanged compared to that of free  $\text{CH}_3\text{ReO}_3$ .

A quantitative single-pulse proton-decoupled  $^{13}\text{C}$  magic angle spinning (MAS) solid-state NMR spectrum of 100%  $^{13}\text{C}$ -labeled  $\text{CH}_3\text{ReO}_3$  on  $\gamma\text{-Al}_2\text{O}_{3-(500)}$  clearly shows one large signal at 31 ppm (78%) and three other signals at 64 (12%), 20 (2%),<sup>[17]</sup> and 10 ppm (8%) (Figures 2 and S2), which indicates clearly that several surface species are in fact present, in contrast to what is suggested by the EXAFS data, which point to the presence of a single species.

We modeled  $\text{CH}_3\text{ReO}_3$  chemisorbed on Lewis acid sites of  $\gamma\text{-Al}_2\text{O}_3$  using periodic calculations. The bulk of  $\gamma\text{-Al}_2\text{O}_3$  contains octahedral (75%,  $\text{Al}_{\text{Oh}}$ ) and tetrahedral (25%,  $\text{Al}_{\text{Td}}$ ) aluminum sites, and the bare surface of fully dehydroxylated alumina is therefore composed of three-coordinate aluminum ( $\text{Al}_{\text{III}}$ , Figure 3a) and truncated octahedral aluminum ( $\text{Al}_{\text{Oh}}$ ), either four- ( $\text{Al}_{\text{IV}}$ , Figure 3b) or five-coordinate ( $\text{Al}_{\text{V}}$ , Figure 3c).<sup>[18–20]</sup> Therefore, on  $\gamma\text{-}$

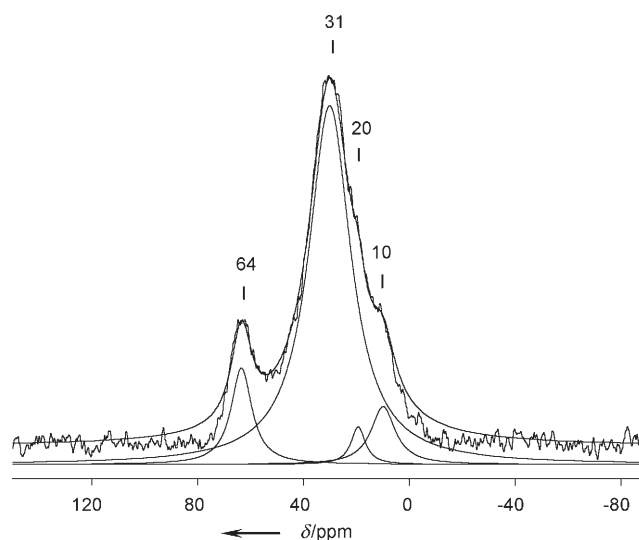


**Figure 2.** Direct proton-decoupling solid-state NMR spectrum of  $^{13}\text{C}$ -labeled  $\text{CH}_3\text{ReO}_3$  on  $\gamma\text{-Al}_2\text{O}_{3-(500)}$  under MAS of 10 kHz and pulse angle of  $45^\circ$ . The number of scans was 5000, and the recycle delay was set to 10 s.

$\text{Al}_2\text{O}_3$  partially hydroxylated at  $500^\circ\text{C}$ , various types of OH groups ( $4\text{OHnm}^{-2}$ ) and Al Lewis acid sites ( $\text{Al}_{\text{III}}$ ,  $\text{Al}_{\text{IV}}$ , and  $\text{Al}_{\text{V}}$ ) are present. We have recently shown, from the reactivity of  $\gamma\text{-Al}_2\text{O}_{3-(500)}$  with  $\text{H}_2$  and  $\text{CH}_4$ , that hydration is not uniform

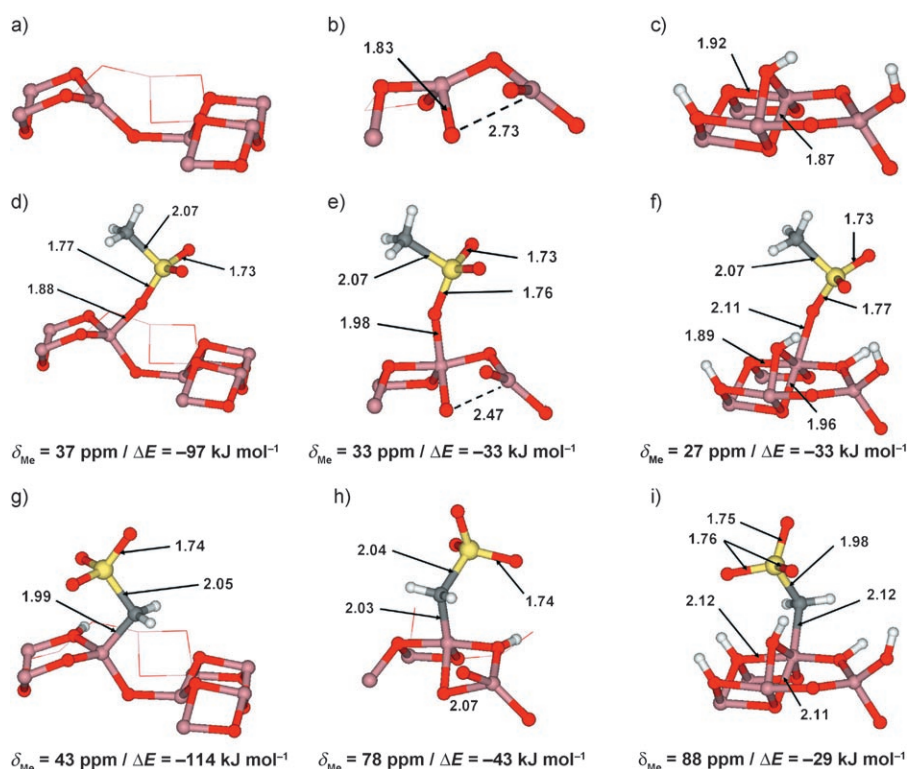


**Figure 3.** Structures of representative aluminum Lewis acid sites (a–c), the corresponding complexes with  $\text{CH}_3\text{ReO}_3$  coordinated to the Al sites (d–f), and the corresponding complexes resulting from heterolytic splitting of the methyl group of  $\text{CH}_3\text{ReO}_3$  on the Al sites (g–i). Relevant bond lengths given in Å. O red, Al pink, C gray, Re yellow, H white. Only a small number of atoms of the periodic surface slab in the vicinity of the grafting site are shown for clarity.  $\delta_{\text{Me}}$  = calculated chemical shift of the methyl substituent relative to  $\text{Me}_4\text{Si}$ , and  $\Delta E$  = adsorption energy. a, d, g)  $\text{Al}_{\text{III}}$  from bulk  $\text{Al}_{\text{Td}}$ ; b, e, h)  $\text{Al}_{\text{IV}}$  from bulk  $\text{Al}_{\text{Oh}}$ ; c, f, i)  $\text{Al}_{\text{V}}$  (from hydration of  $\text{Al}_{\text{IV}}$ ).

and that low-coordinate dehydrated  $\text{Al}_{\text{III}}$  (from bulk  $\text{Al}_{\text{Td}}$ , Figure 3a) and  $\text{Al}_{\text{IV}}$  (from bulk  $\text{Al}_{\text{Oh}}$ , Figure 3b) are present as surface defects.<sup>[20]</sup>  $\text{Al}_{\text{III}}$  ( $0.03 \text{ nm}^2$ ) reacts with  $\text{H}_2$  and  $\text{CH}_4$ ,  $\text{Al}_{\text{IV}}$  ( $0.04 \text{ nm}^2$ ) only with  $\text{H}_2$ , while regular  $\text{Al}_{\text{V}}$  Lewis acid sites (ca.  $4 \text{ nm}^2$ , Figure 3c) react with neither of these molecules. We therefore studied the structure and the associated spectroscopic properties of surface species resulting from the reaction of  $\text{CH}_3\text{ReO}_3$  at various Lewis acid sites (Figure 3d–i).

First, coordination of  $\text{CH}_3\text{ReO}_3$  through an oxo ligand on these Lewis acid sites is exoenergetic, with reaction energies ranging from  $-97$  ( $\text{Al}_{\text{III}}$ ) to  $-33 \text{ kJ mol}^{-1}$  ( $\text{Al}_{\text{V}}$ ; Figure 3d–f). Coordination has only a small effect on the geometries at Re and Al: the lengths of Re–C and Re–O bonds not involved in coordination remain unchanged, and the Re–O bond length of the Re=O bound to Al is only slightly elongated, by 2%. Moreover, the calculated  $^{13}\text{C}$  chemical shifts for the methyl ligand range from 27 to 37 ppm, slightly downfield from those of free  $\text{CH}_3\text{ReO}_3$  ( $\delta_{\text{exptl}} = 17$ ,  $\delta_{\text{calcd}} = 15 \text{ ppm}$ ).

Second,  $\text{CH}_3\text{ReO}_3$  can also react with these Lewis acid sites through C–H activation of its methyl group, and the resulting surface species are more stable than the separate reactants, regardless of the coordination mode at Al, with energies ranging from  $-114$  to  $-29 \text{ kJ mol}^{-1}$  (Figure 3g–i). The calculated  $^{13}\text{C}$  chemical shift of  $\text{CH}_3\text{ReO}_3$  activated on  $\text{Al}_{\text{III}}$  is 43 ppm (Figure 3g) and close to those of the coordinated compounds (see above). In contrast,  $\delta_{\text{Me}}$  of surface species resulting from C–H activation on  $\text{Al}_{\text{Oh}}$  are shifted downfield in the range 78–88 ppm (Figure 3h, i), so the peak observed at 64 ppm can be attributed to  $\text{Al}_{\text{Oh}}\text{--CH}_2\text{ReO}_3$  species. Additionally, grafting by C–H activation generates surface hydroxy groups, hydrogen-bonded to surface Al–O species, and this is also consistent with the appearance of  $\text{Al}_{\text{OH}}$  bands at lower wavenumber in the IR spectrum (Figure 1).

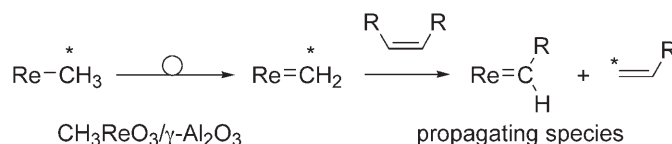
Note that the calculated Re–C and Re=O bond lengths in  $\text{Al}_{\text{S}}\text{--CH}_2\text{ReO}_3$  are close to those in free  $\text{CH}_3\text{ReO}_3$  or in  $\text{CH}_3\text{ReO}_3$  coordinated to Lewis acid sites via the oxo ligands. This explains why the observed EXAFS data can be consistent with a unique Re environment (all the species have similar Re–C and Re–O bond lengths), while numerous surface species are evidenced by NMR spectroscopy. While EXAFS is a powerful tool to determine surface structures, it only provides an average structure and cannot be used to distinguish small differences between several surface sites with similar coordination environments around the metal center.

Considering the surface density of the various types of Al Lewis acid sites, the integration of the observed NMR signals and the  $\delta_{\text{Me}}$  values of various possible surface species, the major surface species ( $1.05 \text{ nm}^2$ ), associated with NMR signals observed around 30 ppm are mainly  $\text{CH}_3\text{ReO}_3$  units coordinated to Lewis acid sites, and the minor species ( $0.15 \text{ nm}^2$ ) correspond to  $\text{Al}_{\text{Oh}}\text{--CH}_2\text{ReO}_3$  units.

$\text{CH}_3\text{ReO}_3/\gamma\text{-Al}_2\text{O}_{3-(500)}$  transforms 500 equiv of propene into a thermodynamic mixture of ethene and 2-butenes in less than 1 h with an initial turnover frequency of  $11 \text{ TON min}^{-1}$ , but the structure of the active site and the importance of the methyl ligand remain to be understood at a molecular

level.<sup>[10,12,13]</sup> We therefore investigated the reaction of several olefins with  $\text{CH}_3\text{ReO}_3$  supported on  $\gamma$ -alumina in order to understand the initiation step.

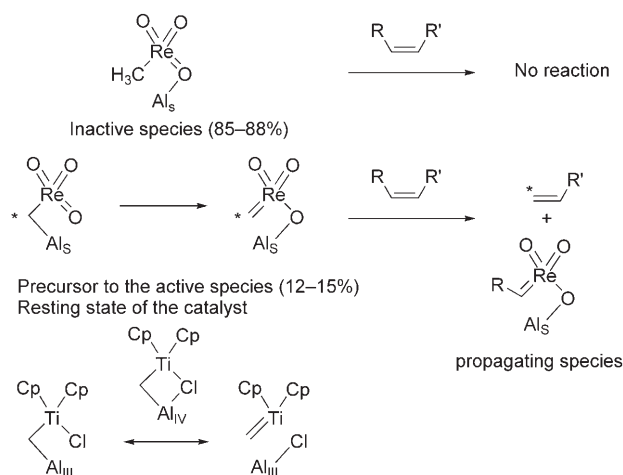
After reaction of  $\text{CH}_3\text{ReO}_3/\gamma\text{-Al}_2\text{O}_{3-(500)}$  with 0.53 equiv of  $^{13}\text{C}$ -labeled ethene for 15 h, 0.40 equiv of ethene was detected, of which 28% was  $^{13}\text{C}$ -monolabeled. Besides ethene, a mixture of  $^{13}\text{C}$ -labeled propene isotopomers was formed (0.015 equiv), probably by decomposition of the metallacyclobutane intermediate.<sup>[21]</sup> Considering a mass balance of 80% and the nonquantitative exchange due to the small amount of ethene per Re active site,  $\text{CH}_3\text{ReO}_3/\gamma\text{-Al}_2\text{O}_{3-(500)}$  contains about 14–15% of active sites. Reverse titration of the active sites by contacting  $\text{CH}_3\text{ReO}_3/\gamma\text{-Al}_2\text{O}_{3-(500)}$ , previously treated with dilabeled ethene, with unlabeled ethene gave  $^{13}\text{C}$ -monolabeled ethene in an amount which also corresponded to about 14–15%. This shows that about 14–15% of the methyl groups are involved in the formation of the propagating carbene species (Scheme 1,  $\text{R} = \text{H}$ ). The involvement of the methyl group of  $\text{CH}_3\text{ReO}_3$  was further confirmed by contacting 99%  $^{13}\text{C}$ -labeled  $\text{CH}_3\text{ReO}_3/\gamma\text{-Al}_2\text{O}_{3-(500)}$  with 11 equiv of (*Z*)-stilbene, which gave (*E*)-stilbene and 0.10 equiv of styrene, 98%  $^{13}\text{C}$ -monolabeled (Scheme 1,  $\text{R} = \text{Ph}$ ).



**Scheme 1.** Mechanistic rational of the metathesis on  $\text{CH}_3\text{ReO}_3/\gamma\text{-Al}_2\text{O}_3$ .

Furthermore, the solid-state  $^{13}\text{C}$  cross-polarization (CP) MAS NMR spectrum of  $\text{CH}_3\text{ReO}_3/\gamma\text{-Al}_2\text{O}_{3-(500)}$  contacted with 0.53 equiv of 100%  $^{13}\text{C}$ -dilabeled ethene showed that the major signal results from a sharp increase of the peak at 66 ppm, previously attributed to  $\text{Al}_{\text{Oh}}\text{CH}_2\text{ReO}_3$  (Figure S3a, b). Other signals also appeared, and they are attributed to physisorbed olefins (144 ppm) and olefin oligomers (31, 21, and 11 ppm), because the same signals appear on contacting  $\gamma\text{-Al}_2\text{O}_3$  with  $^{13}\text{C}$ -dilabeled ethene (Figure S4). Noteworthy, integration of the signal at 64 ppm in the  $^{13}\text{C}$  NMR spectrum of  $^{13}\text{C}$ -labeled  $\text{CH}_3\text{ReO}_3/\gamma\text{-Al}_2\text{O}_{3-(500)}$  (12%, Figure 2) is fully consistent with the titration of this site with  $^{13}\text{C}$ -labeled ethene (14–15%). Note that no signal at lower fields (150–400 ppm range), typical of carbene ligands, was observed (Figure S3c). Therefore,  $\text{Al}_{\text{Oh}}\text{CH}_2\text{ReO}_3$  is the stable form of the active site of the catalyst, which probably generates the necessary carbene in situ during metathesis, and thus this system corresponds to a Re-based heterogeneous equivalent of the Tebbe reagent (Scheme 2).<sup>[22,23]</sup>

In conclusion, for  $\text{CH}_3\text{ReO}_3$  on  $\gamma\text{-Al}_2\text{O}_{3-(500)}$ , a highly efficient olefin metathesis catalyst, the major surface species (85–86%) correspond to interaction of the oxo ligand of  $\text{CH}_3\text{ReO}_3$  with surface Lewis acid sites of alumina, but these are inactive for olefin metathesis. The active site,  $\text{Al}_{\text{Oh}}\text{CH}_2\text{ReO}_3$ , is in fact a minor species (14–15%), and results from C–H activation of the methyl ligand of  $\text{CH}_3\text{ReO}_3$  on  $\gamma$ -alumina. Thus, the major observed surface species is not



**Scheme 2.** Proposed active sites for  $\text{CH}_3\text{ReO}_3$  supported on  $\gamma\text{-Al}_2\text{O}_3$ .

responsible for the catalytic event, and therefore careful use of a combination of several techniques (in particular thorough modeling and labeling experiments) is required to understand the structure of working catalysts at a molecular level.

Received: January 16, 2007  
Published online: April 5, 2007

**Keywords:** density functional calculations · heterogeneous catalysis · metathesis · rhenium · surface chemistry

- [1] C. Cop  ret, M. Chabanas, R. Petroff Saint-Arroman, J.-M. Basset, *Angew. Chem.* **2003**, *115*, 164; *Angew. Chem. Int. Ed.* **2003**, *42*, 156.
- [2] D. G. H. Ballard, *Adv. Catal.* **1973**, *23*, 263.
- [3] T. J. Marks, *Acc. Chem. Res.* **1992**, *25*, 57.
- [4] C. Cop  ret, J. P. Candy, J. M. Basset, *Top. Organomet. Chem.* **2005**, *16*, 151.
- [5] a) M. Chabanas, A. Baudouin, C. Cop  ret, J.-M. Basset, *J. Am. Chem. Soc.* **2001**, *123*, 2062; b) C. Cop  ret, *New J. Chem.* **2004**, *28*, 1; c) F. Blanc, M. Chabanas, C. Cop  ret, B. Fenet, E. Herdweck, *J. Organomet. Chem.* **2005**, *690*, 5014; d) F. Blanc, C. Cop  ret, J. Thivolle-Cazat, J.-M. Basset, A. Lesage, L. Emsley, A. Sinha, R. R. Schrock, *Angew. Chem.* **2006**, *118*, 1238; *Angew. Chem. Int. Ed.* **2006**, *45*, 1216; e) B. Rhers, A. Salameh, A. Baudouin, E. A. Quadrelli, M. Taoufik, C. Cop  ret, F. Lefebvre, J.-M. Basset, X. Solans-Monfort, O. Eisenstein, W. W. Lukens, L. P. H. Lopez, A. Sinha, R. R. Schrock, *Organometallics* **2006**, *25*, 3554; f) F. Blanc, J. Thivolle-Cazat, J.-M. Basset, C. Cop  ret, A. S. Hock, Z. J. Tonzetich, R. R. Schrock, *J. Am. Chem. Soc.* **2007**, *129*, 1044.
- [6] a) W. A. Herrmann, F. E. K  hn, *Acc. Chem. Res.* **1997**, *30*, 169; b) C. C. Romao, F. E. K  hn, W. A. Herrmann, *Chem. Rev.* **1997**, *97*, 3197; c) F. E. K  hn, A. Scherbaum, W. A. Herrmann, *J. Organomet. Chem.* **2004**, *689*, 4149.
- [7] W. A. Herrmann, W. Wagner, U. N. Flessner, U. Volkhardt, H. Komber, *Angew. Chem.* **1991**, *103*, 1704; *Angew. Chem. Int. Ed. Engl.* **1991**, *30*, 1648.
- [8] A. W. Moses, N. A. Ramsahye, C. Raab, H. D. Leifeste, S. Chattopadhyay, B. F. Chmelka, J. Eckert, S. L. Scott, *Organometallics* **2006**, *25*, 2157.
- [9] A. M. J. Rost, H. Schneider, J. P. Zoller, W. A. Herrmann, F. E. K  hn, *J. Organomet. Chem.* **2005**, *690*, 4712.
- [10] R. Buffon, A. Choplin, M. Leconte, J. M. Basset, R. Touroude, W. A. Herrmann, *J. Mol. Catal.* **1992**, *72*, L7.
- [11] A. Malek, G. Ozin, *Adv. Mater.* **1995**, *7*, 160.
- [12] L. J. Morris, A. J. Downs, T. M. Greene, G. S. McGrady, W. A. Herrmann, P. Sirsch, O. Groppen, W. Scherer, *Chem. Commun.* **2000**, 67.
- [13] L. J. Morris, A. J. Downs, T. M. Greene, G. S. McGrady, W. A. Herrmann, P. Sirsch, W. Scherer, O. Groppen, *Organometallics* **2001**, *20*, 2344.
- [14] X. Solans-Monfort, J.-S. Filhol, C. Cop  ret, O. Eisenstein, *New J. Chem.* **2006**, *30*, 842.
- [15] J. Joubert, F. Delbecq, P. Sautet, E. Le Roux, M. Taoufik, C. Thieuleux, F. Blanc, C. Cop  ret, J. Thivolle-Cazat, J.-M. Basset, *J. Am. Chem. Soc.* **2006**, *128*, 9157.
- [16] W. A. Herrmann, W. Scherer, R. W. Fischer, J. Bl  mel, M. Kleine, W. Mertin, R. Gruehn, J. Mink, H. Boysen, C. C. Wilson, R. M. Ibberson, L. Bachmann, M. Mattner, *J. Am. Chem. Soc.* **1995**, *117*, 3231.
- [17] This peak was introduced in the deconvolution because it is more clearly observed by CP/MAS (see Figure S2).
- [18] M. Digne, P. Sautet, P. Raybaud, P. Euzen, H. Toulhoat, *J. Catal.* **2002**, *211*, 1.
- [19] M. Digne, P. Sautet, P. Raybaud, P. Euzen, H. Toulhoat, *J. Catal.* **2004**, *226*, 54.
- [20] J. Joubert, A. Salameh, V. Krakoviack, F. Delbecq, P. Sautet, C. Cop  ret, J. M. Basset, *J. Phys. Chem. B* **2006**, *110*, 23944.
- [21] W. C. P. Tsang, K. C. Hultzs, J. B. Alexander, P. J. Bonitatebus, Jr., R. R. Schrock, A. H. Hoveyda, *J. Am. Chem. Soc.* **2003**, *125*, 2652.
- [22] F. N. Tebbe, G. W. Parshall, G. S. Reddy, *J. Am. Chem. Soc.* **1978**, *100*, 3611.
- [23] F. N. Tebbe, G. W. Parshall, D. W. Ovenall, *J. Am. Chem. Soc.* **1979**, *101*, 5074.